



# Spectroscopic measurement of kinetic energy of sputtered boron in electron cyclotron resonance plasma

Yoshifumi Ito<sup>\*</sup>, Noboru Nakano, Tutomu Yoshidome, Michiro Isobe, Masahiro Nishikawa

*Department of Electromagnetic Energy Engineering, Faculty of Engineering, Osaka University, 2-1 Yamadaoka, Suita, Osaka 565, Japan*

## Abstract

A new diagnostic method for measurement of the kinetic energy of sputtered boron in plasma using spectroscopic technique has been developed. Boron is sputtered by plasma ions produced by electron cyclotron resonance discharge. Line emissions from the borons are measured in directions both parallel and perpendicular to the boron moving axis using a compact monochromator. Observed emission profiles are analyzed by means of non-linear least square fitting and  $E_{\text{peak}}$ , at which the resultant profile  $h_M(E_z)$  has a peak value, is inferred, where surface binding energy  $U_s$ , is nearly equal to  $4 \times E_{\text{peak}}$ . The values  $E_{\text{peak}}$  of the boron sputtered by helium, neon, and argon ions with energy of 2 keV are 1.5–2.0 eV, 0.95–1.3 eV and 1.5–1.7 eV, respectively.

*Keywords:* Low  $Z$  wall material; Neutral particle diagnostic; Line emission diagnostic

## 1. Introduction

Boronization has been applied to tokamak devices for good wall conditioning of the inner wall and has easily yielded good plasma discharges. The boron coating on the wall always suffers from the bombardment of charge exchange neutrals with energy less than a few keV escaping from the plasmas. Sputtering yield, energy of the sputtered boron and its distribution in space are important in order to understand the behavior of the sputtered borons in the plasmas.

The energy (or velocity) distribution of the sputtered atoms has been measured by means of a time-of-flight method [1], a laser-induced fluorescence (LIF) method [2] or an electrostatic analysis method after post-ionization [3]. The LIF spectroscopy has been applied to the measurement of the velocity distribution of sputtered boron [4–6]. Since those methods are not available for our apparatus, we have developed a new diagnostic method to measure the kinetic energy of sputtered boron in the plasma using spectroscopic technique. In this report, we present the new

diagnostics together with the procedure of data analysis and show the experimental results of the energy of borons sputtered by ions produced by electron cyclotron resonance (ECR) discharges.

## 2. Experimental

Since boron sputtering experiments using plasma ions produced by the ECR discharge with 2.45 GHz microwave have already been reported in Ref. [7], only the experimental conditions in this study are given here. Fig. 1 shows the cross-sectional view at the resonance region of the ECR discharge, where the sputtering experiments are done. The base pressure in the vacuum vessel is about  $8 \times 10^{-7}$  Torr. Working gases for the ECR discharge are helium with the filling gas pressure  $P$  of 5.7–46 mTorr, neon with 3.2–25 mTorr and argon with 1.5–5.8 mTorr, and input power of the microwave is 220 W. The electron density  $n_e$  and the temperature  $T_e$  of the plasma in the resonance region are  $n_e = (0.5\text{--}1.5) \times 10^{12} \text{ cm}^{-3}$ ,  $T_e = 5\text{--}6 \text{ eV}$  for He,  $n_e = (0.8\text{--}1.6) \times 10^{12} \text{ cm}^{-3}$ ,  $T_e = 4\text{--}6 \text{ eV}$  for Ne, and  $n_e = (1.2\text{--}1.8) \times 10^{12} \text{ cm}^{-3}$ ,  $T_e = 3\text{--}4.5 \text{ eV}$  for Ar, respectively. Two kinds of solid boron are used as the target boron: small piece of solid boron, about  $1 \times 2 \times 3 \text{ mm}^3$ ,

<sup>\*</sup> Corresponding author. Tel.: +81-770 24 2300; fax: +81-770 24 2303; e-mail: yito@mitene.or.jp.

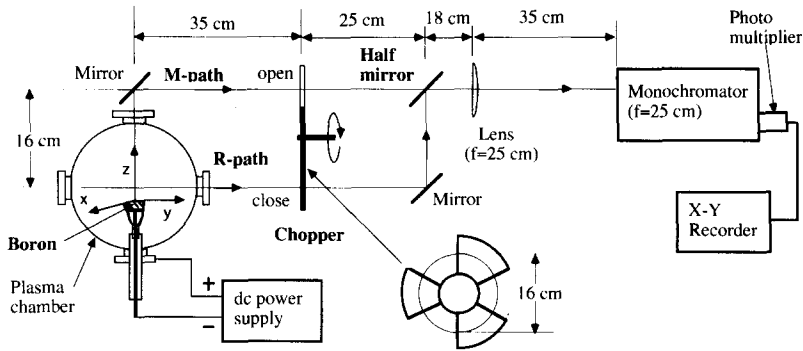


Fig. 1. Optical system for measurement of sputtered boron energy.

with the purity of 99.9% and boron powder with grains of 40 μm diameter with the purity of 99%. Diameter of the target boron surface facing to the plasma is 2 cm. The distance between the center of vacuum vessel and the target surface is about 2 cm. The negative voltage applied to the electrode of the target boron is settled to be constant of -2 kV through the experiments. Thus, helium, neon or argon ions with the energy of 2 keV strike the boron surface in normal direction.

The sputtered boron, moving away from the target, travels in a direction with cosine-like distribution in space. The boron in the plasma emits photons due to electron impact excitation and the wavelength of the emission light from the moving borons is shifted due to the Doppler effect. Fig. 1 shows a schematic drawing of an optical arrangement for the measurements of the boron energy together with coordinate system used here. The direction perpendicular to the target surface is chosen as the z-axis, where the origin is the center of the surface. The line emissions from the sputtered boron in two directions, parallel and perpendicular to the z-axis, are introduced into a monochromator using a half mirror and a lens. The former emission light is called 'M-light' and the latter one 'R-light'. The deposition profiles of the thin films prepared by the sputtered boron on a substrate at z = 2–4 cm indicate that the borons travel symmetrically against the z-axis with cosine-like distribution. The wavelength center of the characteristic line emission can be determined from the line profile of R-light which is Doppler free one. A light chopper, composed of a motor and a circular plate of three open and close regions with same area, is placed so that the emissions passing through each optical path of M- and R-lights can be observed alternatively during one wavelength scan of the monochromator.

A compact monochromator with focus distance of 25 cm and F-value of 4.3 is used here. The instrumental function  $I(\lambda)$  of the monochromator is determined from the emission line profile measured by a standard lamp. The full half width of  $I(\lambda)$  is about 0.83 Å at 3888 Å. The resonance line of the boron atoms (B1; 2s<sup>2</sup>3s-2s<sup>2</sup>2p), which is a doublet line with each a center wavelength of

2496.78 Å ( $\lambda_1$ ) and 2497.73 Å ( $\lambda_2$ ), are used since it is strong enough to be identified easily in the wavelength region around 2500 Å. The line profiles of the emission from the carbon (C1;  $\lambda_0 = 2478.6$  Å), which is contained in the plasma as the impurity, are also measured in the same optical arrangement as shown in Fig. 1. In the profiles of the line emission from the carbon, the central wavelength of M-light coincides with that of R-light within this experimental accuracy.

### 3. Fitting function for data analysis

The velocity distribution  $f(v_z)$  of the sputtered atoms at the distance z from the surface with radius R is given by Bay et al. [2] using Thompson distribution,

$$f(v_z) \propto \left(1 + \frac{v_z^2}{v_s^2}\right)^{-2} - \left(1 + \frac{z^2 + R^2}{z^2} \cdot \frac{v_z^2}{v_s^2}\right)^{-2} \quad (1)$$

Here  $U_s (\equiv mv_s^2/2)$  is the surface binding energy, which is one of the fitting parameters to be determined in data fitting procedure. Emission profile  $h_M(\lambda)$  of M-light to enter the monochromator is found after integration of Eq. (1) along the line of sight in the plasma,

$$h_M(\lambda) \propto \frac{\alpha}{(\alpha + 1)^3} \left[ \frac{3}{\sqrt{\beta}} \tan^{-1} \left( \frac{d_m}{\sqrt{\beta}} \right) - \frac{d_m}{d_m^2 + \beta} \right], \quad (2)$$

where  $\alpha (= E_z/U_s = v_z^2/v_s^2) = (\lambda - \lambda_0)^2/(\lambda_s - \lambda_0)^2 = \Delta\lambda^2/\Delta\lambda_s^2$ ,  $\beta = \alpha(\alpha + 1)$ , and  $d_m = z_m/R$ . Here,  $z_m$  is the maximum distance to the target and, accordingly, the upper bound for the integration. When  $d_m \rightarrow \infty$ , Eq. (2) is reduced to the simple equation

$$h_M(\lambda) = \frac{\alpha^{1/2}}{(\alpha + 1)^{5/2}} \quad (3)$$

The function  $f(v_z)$  decreases rapidly with increase of z, being nearly in proportion to  $z^{-2}$ , so Eq. (3) is valid for

$d_m \geq 6$ . In this experiments of  $d_m \approx 9$ , Eq. (3) holds. The function  $h_M(\lambda)$  is unsymmetrical one which has a peak value at  $\Delta\lambda_{\text{peak}} (\approx 0.5 \times \Delta\lambda_s)$  with the full half width  $\Delta\lambda_{s,1/2}$ . The typical values of  $\Delta\lambda_{\text{peak}}$  and  $\Delta\lambda_{s,1/2}$  are about 0.04 Å and 0.08 Å, respectively. Accuracy of the transition probability of resonance doublet line of the boron atoms reported is less than 50% [8]. So, the following line profile  $H_M(\lambda)$  is adopted for M-light:

$$H_M(\lambda) = A \cdot h_M(\alpha_1) + B \cdot h_M(\alpha_2), \quad (4)$$

where  $\alpha_1 = (\lambda - \lambda_1)/(\lambda_s - \lambda_1)$  and  $\alpha_2 = (\lambda - \lambda_2)/\lambda_s - \lambda_2$ , and  $A$  and  $B$  are the relative intensities of each line. The fitting function  $F_M(\lambda)$  of the observed data for M-light is found after the convolution integral of  $H_M(\lambda)$  and the instrumental function  $I(\lambda)$ .

Emission profile  $h_R(\lambda)$  of R-light to enter the monochromator is assumed to be a form of  $\delta(\lambda - \lambda_0)$ . Emission profile of R-light can be considered to be symmetric against the line center because of the cosine-like space-distribution of the boron, being symmetric against the  $z$ -axis. Since the line broadening of R-light is expected to be in the same order of (or narrower than) that of M-light the full half width of  $h_R(\lambda)$  is considered to be less than 0.1 of that of  $I(\lambda)$ . As the emission profile of R-light is used only for the determination of the wavelength center, the assumption of  $\delta$  function for the R-light profile is suitable in this analysis. Thus, the following fitting function  $F_R(\lambda)$  is given for R-light:

$$F_R(\lambda) = A \cdot I(\lambda - \lambda_1) + B \cdot I(\lambda - \lambda_2). \quad (5)$$

The parameters in data fitting to the function are  $\lambda_1$  (or  $\lambda_2 \equiv \lambda_1 + 0.95$  Å),  $\lambda_s$ ,  $A$ , and  $B$ . The observed data are

fitted using non-linear least squares in two step process; (i) the value of  $\lambda_1$  is derived from use of Eq. (5); (ii)  $\Delta\lambda_s (= \lambda_s - \lambda_1)$  is determined from use of the function  $F_M(\lambda)$ . The resultant parameters yield the energy distribution  $h_M(E_z)$  of the sputtered boron which has a peak value at  $E_z = E_{\text{peak}} (\approx U_s/4)$  with the full half width of about  $4 \times E_{\text{peak}}$ . In this report, value of  $E_{\text{peak}}$  is used as the presentation of the energy of the sputtered boron obtained in various experimental conditions.

#### 4. Results and discussion

Fig. 2 shows an example of the profiles of the boron line emissions obtained in one wavelength scan, where open circles are observed values of M- and R-lights and solid curves are the resultant profiles obtained from the data fitting. Fig. 2 indicates that data are well fitted to the used functions. The wavelength at the peak value in the line profile of M-light is slightly but apparently shifted to blue side against that of R-light. The intensity ratio of M-light to R-light is about 5:2 which agrees well with the boron line-density integrated along the line of sight of the monochromator in the plasmas for M- and R- lights. Here, the space distribution of the boron density is assumed to be cosine distribution with  $z^{-2}$  dependence along  $z$ -axis.

The values  $E_{\text{peak}}$  of the boron sputtered by helium, neon and argon ions are plotted as a function of the filling gas pressure  $P$  in Fig. 3a, b and c, respectively. Here, closed circles are values in case of using the small piece of solid boron and open circles are in case of powder borons. Fig. 3 show that the surface roughness of the target borons

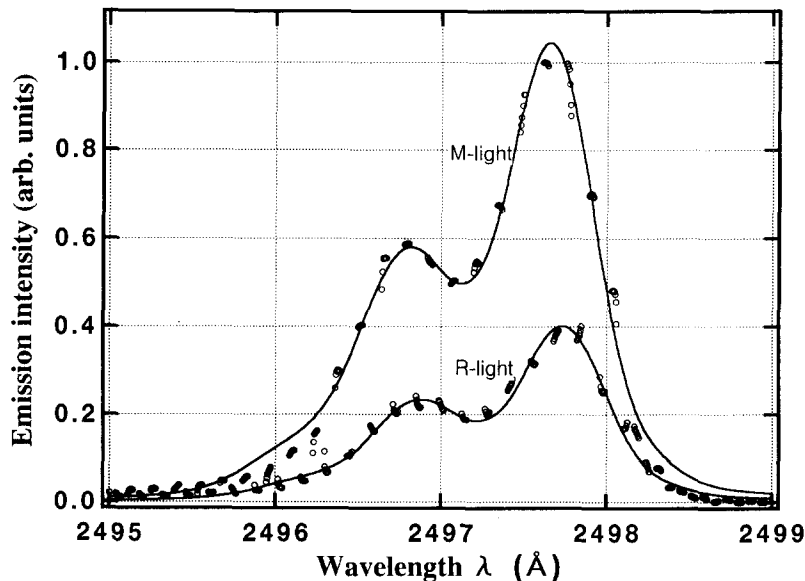


Fig. 2. Emission profiles of the sputtered boron. Here, open circles are the observed values and solid curves are the resultant profiles obtained from the data fitting.

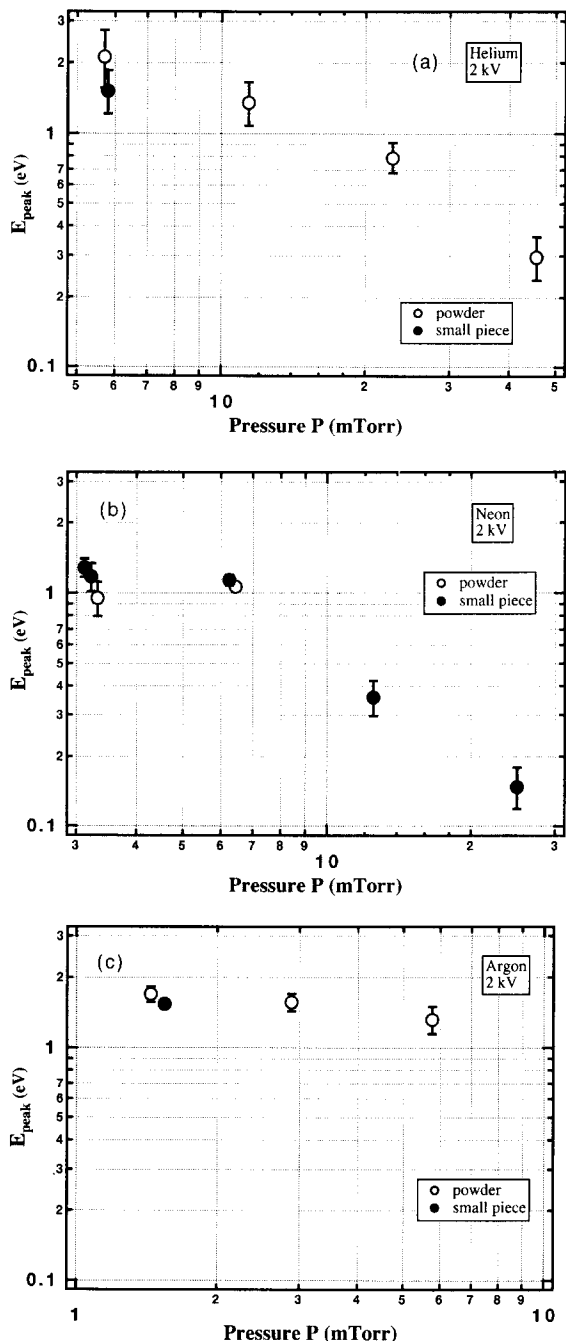


Fig. 3.  $E_{\text{peak}}$  of the sputtered boron as a function of gas pressure  $P$ , where sputtering ions are (a) helium, (b) neon, and (c) argon with energy of 2 keV. Here,  $E_{\text{peak}}$  is the energy at which the distribution is given in Eqs. (2) and (3) has a peak value, and the surface binding energy  $U_s$  is about  $4 \times E_{\text{peak}}$ . Closed and open circles are in case of the small piece of solid boron and powder borons, respectively. Error bars show confidence interval in the case of confidence coefficient of 0.9.

does not effect hardly on  $E_{\text{peak}}$ .  $E_{\text{peak}}$  is nearly constant in the pressure region of  $P < 7\text{--}10$  mTorr, while the  $E_{\text{peak}}$  decreases with the pressure in  $P > 10$  mTorr. The observed emission signals mainly come from the boron in the region near the target surface due to the density distribution of the sputtered boron with the  $z^{-2}$  dependence. The constant values of  $E_{\text{peak}}$  in  $P < 7$  mTorr imply that the assumption of collision free of the boron atoms, which is tacitly used in the fitting functions, is reasonable in this pressure region. The mean free path of the boron atoms due to the elastic collision with neutral particles is roughly estimated to be 2 cm for  $P = 10$  mTorr. The decrease of  $E_{\text{peak}}$  in  $P > 7$  mTorr may be ascribed to the elastic collision of the boron with the neutrals. Further discussion about  $E_{\text{peak}}$  in  $P > 7$  mTorr, however, is impossible because the collision effect of the boron in the plasma is not taken into account in this analysis and, so we focus only on  $E_{\text{peak}}$  in  $P < 7$  mTorr below.

Fig. 3 shows that the values of  $E_{\text{peak}}$  are 1.5–2.0 eV for He, 0.95–1.3 eV for Ne and 1.5–1.7 eV for Ar. The surface binding energy  $U_s$  inferred here is about  $4 \times E_{\text{peak}}$  which is the same order of the sublimation energy (5.8 eV) of the boron in solid state [9]. Rowekamp et al. [5] measured the velocity distribution of the boron sputtered by argon ion beam with energy of 1 keV by LIF spectroscopy and obtained the surface binding energy  $U_s$  of 5.6 eV by fitting the experimental curve to the Thompson distribution, where  $\text{B}_4\text{C}$  was used as the target. However, LIF result reported by Pasch et al. [6] showed that the fluorescence signals of the boron sputtered from an a-C/B:H target deviated strongly from the Thompson distribution with  $U_s = 5.6$  eV. The binding energy  $U_s$  of the pure boron target inferred in this experiment has weak dependence on the species of the injecting ions:  $U_s$  in cases of helium and argon is slightly higher than that in case of neon. This may originate in the mass effect of the injected ions on the collision process between ions and boron in the target. However, detailed explanation about the difference of  $U_s$  is not clear and, so further study about the boron sputtering phenomena seems to be required now.

## 5. Conclusion

New diagnostics for the measurement of the kinetic energy of the sputtered boron in the plasma using spectroscopic technique have been developed. Helium, neon and argon plasmas are produced by ECR discharge in wide region of the filling gas pressure, and the ions with energy of 2 keV strike the pure boron target. The line emissions from the sputtered boron in the plasma are observed by use of a compact monochromator and the data are fitted using non-linear least squares to the functions obtained by the

convolution integral. The values of  $E_{\text{peak}}$  in  $P < 7$  mTorr is nearly constant; 1.5–2.0 eV for He, 0.95–1.3 eV for Ne and 1.5–1.7 eV for Ar, where  $E_{\text{peak}}$  is the energy at which the inferred distribution  $h_M(E_z)$  has a peak value. The surface binding energy  $U_s$  ( $\approx 4 \times E_{\text{peak}}$ ) is slightly higher than (or nearly equal to) the sublimation energy of the boron in solid state.

## References

- [1] R.V. Stuart and G.K. Wehner, J. Appl. Phys. 35 (1964) 1819.
- [2] H.L. Bay, W. Berres and E. Hintz, Nucl. Instrum. Methods 194 (1982) 555.
- [3] J. Dembowski, H. Oechsner and Y. Yamamura, Nucl. Instrum. Methods Phys. Res. B 18 (1987) 464.
- [4] A. Goehlic, M. Rowekamp and H.F. Dobel, J. Nucl. Mater. 176–177 (1990) 1055.5
- [5] M. Rowekamp, A. Goehlic and H.F. Dobel, Appl. Phys. A 54 (1992) 61.
- [6] E. Pasch, P. Bogen and Ph. Mertens, J. Nucl. Mater. 196–198 (1992) 1065.
- [7] Y. Ito, S. Kuriki, M. Saidoh and M. Nishikawa, Jpn. J. Appl. Phys. 33 (1994) 5959.
- [8] W.L. Wiese, M.W. Smith and B.M. Glennon, Atomic Transition Probabilities, Vol. 1, Hydrogen Through Neon, NSRDS-NBS 4 (1966).
- [9] C. Kittel, Introduction to Solid State Physics (Wiley, New York, 1976).